PHYSICAL REVIEW B **75**, 201304(R) (2007)

Enhanced electron-hole interaction and optical absorption in a silicon nanowire

Li Yang,[1] Catalin D. Spataru,[2,3] Steven G. Louie,[2,3] and M. Y. Chou[1]
[1]*School of Physics, Georgia Institute of Technology, Atlanta, Georgia 30332-0430, USA*
[2]*Department of Physics, University of California at Berkeley, California 94720, USA*
[3]*Materials Sciences Division, Lawrence Berkeley, National Laboratory, Berkeley, California 94720, USA*
(Received 8 August 2006; revised manuscript received 13 March 2007; published 23 May 2007)

We present a first-principles study of the correlated electron-hole states in a silicon nanowire of a diameter of 1.2 nm and their influence on the optical absorption spectrum. The quasiparticle states are calculated employing a many-body Green's function approach within the GW approximation to the electron self-energy, and the effects of the electron-hole interaction to optical excitations are evaluated by solving the Bethe-Salpeter equation. The enhanced Coulomb interaction in this confined geometry results in an unusually large binding energy (1–1.5 eV) for the excitons, which dominate the optical absorption spectrum.

DOI: 10.1103/PhysRevB.75.201304 PACS number(s): 73.21.Hb, 78.67.−n, 78.67.Lt, 81.07.Vb

When an electron in a semiconductor is promoted from a valence band to a conduction band, it creates a "hole" in the crystal, which in turns interacts with the excited electron owing to the Coulomb interaction. One needs to go beyond a single-particle picture in order to describe this interaction, which gives rise to the formation of excitons. Excitonic effects are often noticeable in optical absorption studies of semiconductors.[1–3] After including the electron-hole interaction, the calculated optical spectrum is modestly modified in bulk silicon, mostly in the enhancement of the E_1 peak.[2,3] However, because of the weakened screening in a confined geometry, the electron-hole interaction is expected to be much intensified in low-dimensional structures and excitonic effects are found to be crucial in optical absorption studies for nanomaterials. Previous reports in the literature have demonstrated the importance of excitons in carbon and BN nanotubes[4–8] and semiconductor quantum dots.[9]

Semiconductor nanowires have been identified as potential building blocks for nanoscale devices and have attracted wide interest in recent years.[10] In particular, silicon single-crystal nanowires (SiNWs) have been fabricated and their potential in future applications demonstrated.[11–13] The confinement effect on the size-dependent electronic properties is of central interest. This size dependence has been studied from first principles, mostly within the theoretical framework of density functional formalism, and a few one-particle optical absorption results have been reported recently.[14,15] However, without including electron-hole interactions at the same level of accuracy, the optical gap and polarization-dependent absorption spectra remain open questions. Previous empirical studies with effective-mass and tight-binding models suggested significant excitonic features for these nanowires,[16] although no definitive answer was provided because of the approximations used. Experimental data are also limited; certain pronounced peaks in the absorption spectra were observed,[13] but no detailed analysis was provided.

The choice of this nanowire is motivated by the experimental finding that the smallest nanowires (down to a few nanometers in diameter) grew primarily along the [110] direction.[17] In this paper, we report a first-principles study of the correlated electron-hole states and the optical absorption spectrum for a hydrogen-passivated SiNW of a diameter of 1.2 nm, with the wire axis along the [110] direction. Using norm-conserving pseudopotentials[18] and plane waves, we first obtain the electronic ground state and the relaxed atomic structure within density functional theory (DFT) in the local density approximation (LDA).[19] Second, the GW corrections to the quasiparticle energies[20] are calculated. In the final step, we compute the electron-hole-excited states by solving the Bethe-Salpeter equation (BSE) of the two-particle Green's function.[3,21]

In this approach,[3] the electron-hole-excited states are represented by the expansion (suppressing spin indices)

$$|S\rangle = \sum_{k}^{} \sum_{v}^{hole} \sum_{c}^{elec} A^{S}_{vck} a^{\dagger}_{vk} b^{\dagger}_{ck} |0\rangle =: \sum_{k}^{} \sum_{v}^{hole} \sum_{c}^{elec} A^{S}_{vck} |vck\rangle, \quad (1)$$

where $a^{\dagger}$ and $b^{\dagger}$ are the quasiparticle creation operators for a hole and an electron, respectively, while $|0\rangle$ is the many-body ground state. Equation (1) includes a k sum over the Brillouin zone (BZ), a summation over the valence bands (v) for the hole states, and a summation over the conduction bands (c) for the electron states. A^{S}_{vck} is the exciton amplitude obtained by solving the BSE[3,21]

$$(E_{ck} - E_{vk}) A^{S}_{vck} + \sum_{k'v'c'} \langle vck|K^{eh}|v'c'k'\rangle A^{S}_{v'c'k'} = \Omega^{S} A^{S}_{vck}, \quad (2)$$

where K^{eh} is the electron-hole interaction kernel, E_{ck} and E_{vk} are quasiparticle energies for the conduction and valence bands, respectively, and Ω^{s} is the energy of the excitonic state. If we neglect spin-orbit interactions, the one-particle basis functions are the same for spin-up and spin-down quasiparticles. Under this condition, the procedures outlined above can be easily extended to include the spin degree of freedom.[3] In this study we shall concentrate on optical absorption; therefore, only spin singlets will be considered.

To mimic isolated nanowires, we carry out calculations in a hexagonal supercell imposing the periodic boundary condition in the plane perpendicular to the wire axis, with the size of the supercell being more than twice the diameter of the SiNW. Taking into account the periodicity in the axial direction, each unit cell contains 16 silicon and 12 hydrogen atoms. A ball-and-stick model is shown in Fig. 1. The plane-

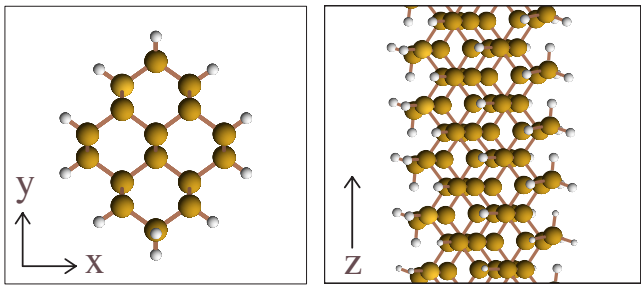

FIG. 1. (Color online) Ball-and-stick model of the hydrogen-passivated silicon nanowire under investigation: top view (left) and side view (right). The large atoms are silicon and small atoms are hydrogen.

wave energy cutoff is set at 12 Ry to ensure total-energy convergence in the ground-state calculation. To avoid long-range Coulomb interactions between wires in adjacent supercells, we use a truncated Coulomb interaction of the form[5]

$$V_c = \frac{1}{r}\theta(\rho - \rho_c)\,\theta(|z| - z_c), \tag{3}$$

where ρ and z are cylindrical coordinates for the relative positions between two particles. The radial cutoff ρ_c is set to be half of the distance between neighboring wires (24 a.u.), while the cutoff z_c along the wire direction is set at 420 a.u. in the exciton calculation, which is much larger than the typical size of the excitons under investigation and smaller than the length scale determined by the k-point sampling. We have used a grid of 32 one-dimensional k points in the DFT and GW calculations to obtain converged quasiparticle energies; 400 bands including 38 valence bands are employed in the self-energy calculation. As discussed previously,[5] the k-point sampling in the BSE step should be much denser than that in the DFT and GW calculations. Hence, the electron-hole interaction kernel K^{eh} is first computed on a coarse k grid (32 k points), then interpolated on a fine grid (192 k points) to get converged results. Twelve valence bands and 12 conduction bands are included in Eq. (1). Equation (2) is diagonalized to obtain the exciton energies Ω^s and electron-hole amplitudes A_{vck}.

Finally, to describe the absorption spectra of the SiNW, we calculate a quantity representing the polarizability per nanowire in units of nm^2:

$$\alpha(\omega) = \frac{4e^2A}{\omega^2}\sum_s |\vec{\lambda}\cdot\langle 0|\vec{v}|S\rangle|^2\delta(\omega - \Omega_s), \tag{4}$$

which is obtained by multiplying the imaginary part of the calculated dielectric susceptibility, $\kappa=(\epsilon-1)/4\pi$, by the cross-sectional area of the supercell A perpendicular to the nanowire axis. The imaginary part of the dielectric function ϵ_2 as a function of energy ω ($\hbar=1$) is evaluated as usual.[3,22]

In Fig. 2 we show the GW quasiparticle band structure along the axial direction. Bulk silicon has an indirect band gap with the conduction-band minima located along the Γ-X direction near X in the BZ. Because of the geometric structure of the specific SiNW considered, two of the bulk ΓX branches are mapped to the $k=0$ point in the one-dimensional (1D) BZ, resulting in a direct band gap induced by confinement in the directions perpendicular to the wire axis. The electron self-energy corrections to the Kohn-Sham eigenvalues are enhanced in the SiNW compared with those in the bulk. Our GW band gap (3.2 eV) is twice the band gap from the LDA calculation (1.6 eV). With this quasiparticle band structure and the corresponding wave functions, we then calculated the one-particle optical absorption spectrum. For consistent comparison with results including excitonic effects, we also included 12 conduction bands and 12 valence bands at this stage of the calculation.

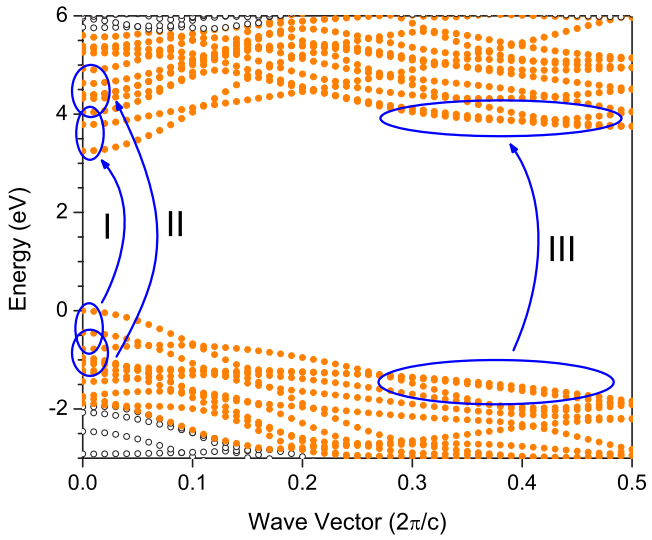

FIG. 2. (Color online) Electronic band structure of the SiNW with GW corrections included. The solid dots represent the bands included in exciton calculations. The marked transition groups I, II, and III are dominant contributors to optical absorption peaks in Fig. 3.

The one-particle $\alpha_2(\omega)$ with the polarization vector of light along the axial direction is shown in the upper panel of Fig. 3. The spectrum includes an artificial broadening of 0.1 eV. The group of transitions labeled by I in Fig. 2 cover the region up to 5 eV, including the first peak at about 4.7 eV labeled by a triangle. It is noted that the optical absorption is only appreciable starting around at least 1 eV above the fundamental gap marked by A. Because of the symmetry of the wave functions, the first few direct transitions have vanishingly small dipole matrix elements, which contribute to a symmetry gap in the optical absorption of the SiNW. This is not surprising since the first few conduction states at $\bar{\Gamma}$ (zone-center point of the 1D BZ of the wire) are connected with the bulk states in the ΓX branches of the Si bulk BZ away from Γ. The degeneracy at the top of the valence bands is also lifted because of the finite size of the SiNW. Given the nature of the states involved, the first peak in the spectrum, labeled by a triangle, is a new feature in the SiNW compared with the bulk resulting from confinement.

The next feature in Fig. 3, labeled by a solid circle, includes two close peaks originating from transitions II and III marked in Fig. 2. They correspond to the E_1 peak in bulk silicon at 3.5 eV, which is blueshifted, enhanced, and split in the SiNW. The bulk E_1 peak is due to transitions in the

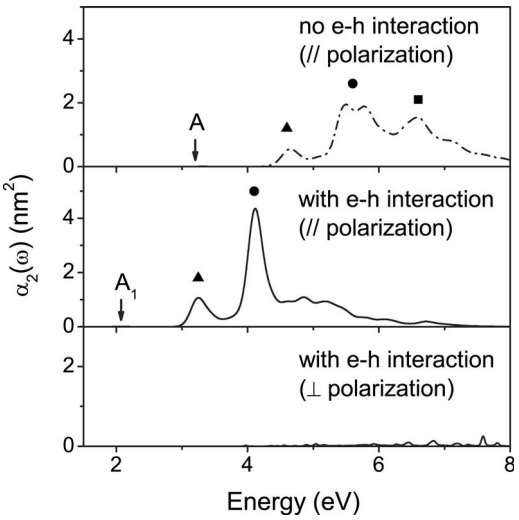

FIG. 3. Absorption spectrum of the silicon nanowire calculated with a smearing width of 0.1 eV. The arrows marked by A and A_1 indicate the fundamental gap and the lowest-energy exciton locations, respectively. The extremely small absorption for polarization perpendicular to the axis illustrates the depolarization effect.

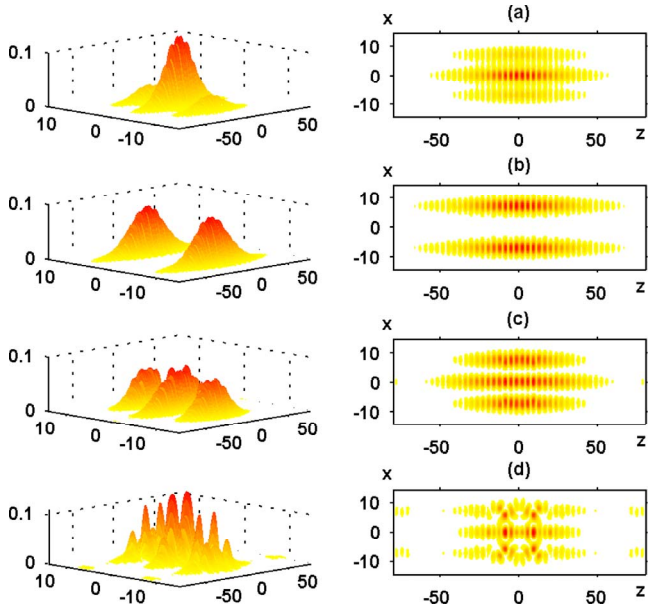

FIG. 4. (Color online) The density of the electron for several excitonic states with the hole fixed at the center of the wire between two nearest-neighbor Si atoms. From top to bottom, four representative states are shown with energy values of 2.1 eV, 3.3 eV, 4.2 eV, and 4.2 eV, respectively. Corresponding cross-section plots on the xz plane are shown on the right, while the three-dimensional plots for the same data are shown on the left. Lengths are in atomic units.

neighborhood of the L point in the bulk BZ between the top valence band and the nearly parallel lowest conduction band in the [111] direction. In the [110] nanowire under consideration, the bulk L points map to either $k=0$ or the zone boundary. Therefore, the corresponding transitions appear around $k=0$ (transitions labeled by II) and between parallel bands in the 1D BZ (transitions labeled by III). The final peak marked by a square is connected with the bulk absorption peak E_2. It consists of many transitions in the SiNW, therefore not labeled in Fig. 2.

After solving the BSE, we obtain the energies and wave functions of the excitonic states. The majority of the solutions are optically inactive. The density of states (DOS) of the excitons, most of which are in the continuum, is similar to the joint density of single-particle states. In contrast, the lowest-energy bound exciton, with an excitation energy of 2.1 eV (well inside the quasiparticle band gap) and marked by A_1 in Fig. 3, has a binding energy of more than 1 eV. This is two orders of magnitude larger than the exciton binding energy in the bulk (14.7 meV). The optical dipole matrix element for this particular bound exciton is very small. Its electron distribution in the xz plane is shown in Fig. 4(a), with the hole fixed at the center of the wire between two nearest-neighbor Si atoms. The "size" is about 40–50 Å, smaller than what is expected for the bulk.

Significant changes are found in the absorption spectrum of the SiNW after the electron-hole interaction is taken into account. The results are shown in the lower two panels of Fig. 3 for polarization along and perpendicular to the wire axis, respectively. For polarization perpendicular to the axial direction, the absorption is suppressed due to the depolarization effect.[23] For polarization parallel to the axial direction, all the features now occur at much lower energies compared with the one-particle result. The electron-hole interaction has created strongly correlated exciton states in symmetry gaps at energy above the fundamental quasiparticle gap, and the oscillator strength of the interband transitions has been predominantly transferred to these bound exciton states, giving rise to new peaks in the spectrum. As a result, the absorption spectrum is dominated by a few new peaks that are very different from those in the single-particle spectrum. We note that, because of the symmetry gaps, the optically active excitons here are bound excitons although they have excitation energy above the fundamental gap.

The peak around 3.3 eV, marked by a triangle, comprises excitons made of primarily a mixture of free electron-hole pairs within group I marked in Fig. 2. The electron distribution for a representative excitonic state is shown in Fig. 4(b) with the hole fixed at the wire center. Again, the distribution is quite localized. The large peak around 4.2 eV, marked by a circle in the middle panel of Fig. 3, is the most dominating feature in the spectrum and is made of mainly two large-amplitude exciton peaks. The first (second) one is composed of combinations of free electron-hole pairs marked by II (III) in Fig. 2. An anomalously high absorption amplitude for these two excitonic states arises from a coherent and constructive superposition of the oscillator strengths of coupled electron-hole configurations within the respective group. The electron distributions for these two states are shown in Fig. 4(c) and 4(d), respectively. The latter contains electron-hole pairs over an extended region of the BZ, yielding a particularly short-ranged bound exciton with large overlap of electron and hole wave functions in real space.

The major finding of the current study—namely, a dominating peak in the optical absorption spectrum associated

with bound exciton states derived from the bulk E_1 peak—is expected to be a general feature for small diameter SiNWs. Hence the spectrum for such SiNWs is characteristically and categorically different from that in the bulk. It demonstrates the ultimate importance of electron-hole interactions in the optical response of these quasi-one-dimensional nanostructures. Quantum confinement modifies the electron and hole wave functions and allows for a larger overlap between them, thus enhancing the interaction. In addition, screening is also largely reduced in the nanowire, owing to the larger quasiparticle gap and a finite diameter surrounded by vacuum. Interestingly, quantum confinement increases the energy gap and moves the one-particle absorption features to higher energies in the nanowire, while the enhanced electron-hole interaction gives rise to large binding energies for the relevant excitons. The two effects are both significant, but affect the spectrum in opposite ways, resulting in a nearly overall cancellation. Therefore, unexpectedly, absorption peaks are still being found in the 3–4-eV range for a SiNW with diameter of as small as 1.2 nm.

In conclusion, we have performed a detailed study of the effects of electron-hole interactions in the optical response of a silicon nanowire from first principles. Because of the quantum confinement effect and reduced dimensionality, the excitonic effect is greatly enhanced. Compared with bulk silicon, significantly different optical spectra dominated by bound exciton peaks are predicted. The binding energy of these excitons is about 1–1.5 eV, much larger than the value of 15 meV in the bulk. The most significant peak for a 1.2-nm silicon nanowire is at 4.2 eV, resulting from bound excitons associated with the E_1 peak in the bulk. This feature of a predominant peak is expected to be a general feature of the optical absorption spectrum of small diameter silicon nanowires.

We note that an independent calculation of the optical properties of Si nanowire was just published.[24] The lowest exciton energy and the most dominant peak for this nanowire are found to be at 1.9 eV and 3.8 eV, respectively, compared with our results of 2.1 eV and 4.2 eV. We believe that the difference arises from the fact that the Coulomb interaction is not truncated in Ref. 24. In our calculation we find the truncation of the long-range Coulomb interaction to be particularly important in order to ensure the convergence of 0.1 eV in the GW band gaps and 0.1 eV in exciton energies.

This work is supported by the National Science Foundation (Grants No. DMR-02-05328, No. DMR-04-39768, and No. SBE-01-23532), the Department of Energy (Grant No. DE-FG02-97ER45632), and the Director, Office of Science, Office of Basic Energy Sciences, Division of Materials Sciences and Engineering, of the U.S. Department of Energy under Contract No. DE-AC02-05CH11231. Computation resources were provided by the San Diego Supercomputing Center (SDSC) and the National Energy Research Scientific Computing Center (NERSC). The support from the Computational Material Science Network (CMSN) of the U.S. Department of Energy is also acknowledged.

[1] W. Hanke and L. J. Sham, Phys. Rev. Lett. **43**, 387 (1979).
[2] M. del Castillo-Mussot and L. J. Sham, Phys. Rev. B **31**, 2092 (1985).
[3] M. Rohlfing and S. G. Louie, Phys. Rev. B **62**, 4927 (2000).
[4] C. D. Spataru, S. Ismail-Beigi, L. X. Benedict, and S. G. Louie, Phys. Rev. Lett. **92**, 077402 (2004).
[5] C. D. Spataru, S. Ismail-Beigi, L. X. Benedict, and S. G. Louie, Appl. Phys. A: Mater. Sci. Process. **78**, 1129 (2004).
[6] E. Chang, G. Bussi, A. Ruini, and E. Molinari, Phys. Rev. Lett. **92**, 196401 (2004).
[7] C.-H. Park, C. D. Spataru, and S. G. Louie, Phys. Rev. Lett. **96**, 126105 (2006); L. Wirtz, A. Marini, and A. Rubio, *ibid.* **96**, 126104 (2006).
[8] F. Wang, Gordana Dukovic, L. E. Brus, and T. F. Heinz, Science **308**, 838 (2005).
[9] I. Vasiliev, S. Ogut, and J. R. Chelikowsky, Phys. Rev. Lett. **86**, 1813 (2001).
[10] For a review, see D. J. Sirbuly, M. Law, H. Yan, and P. Yang, J. Phys. Chem. B **109**, 15190 (2005).
[11] Y. Cui and C. M. Lieber, Science **291**, 851 (2001); X. Duan, Y. Huang, Y. Cui, J. Wang, and C. M. Lieber, Nature (London) **409**, 66 (2001).
[12] A. M. Morales and C. M. Lieber, Science **279**, 208 (1998).
[13] J. D. Holmes, K. P. Johnston, R. C. Doty, and B. A. Korgel, Science **287**, 1471 (2000).
[14] X. Y. Zhao, C. M. Wei, L. Yang, and M. Y. Chou, Phys. Rev. Lett. **92**, 236805 (2004).
[15] A. N. Kholod, V. L. Shaposhnikov, N. Sobolev, V. E. Borisenko, F. A. D'Avitaya, and S. Ossicini, Phys. Rev. B **70**, 035317 (2004).
[16] G. D. Sanders and Y.-C. Chang, Phys. Rev. B **45**, 9202 (1992).
[17] Wu *et al.*, Nano Lett. **4**, 433 (2004).
[18] N. Troullier and J. L. Martins, Phys. Rev. B **43**, 1993 (1991).
[19] W. Kohn and L. J. Sham, Phys. Rev. **140**, A1133 (1965).
[20] M. S. Hybertsen and S. G. Louie, Phys. Rev. B **34**, 5390 (1986).
[21] G. Strinati, Phys. Rev. Lett. **49**, 1519 (1982); Phys. Rev. B **29**, 5718 (1984).
[22] M. L. Cohen and J. R. Chelikowsky, *Electronic Structure and Optical Properties of Semiconductors*, 2nd ed. (Springer-Verlag, New York, 1988).
[23] T. Ando, J. Phys. Soc. Jpn. **66**, 1066 (1997); M. Machon, S. Reich, C. Thomsen, D. Sanchez-Portal, and P. Ordejon, Phys. Rev. B **66**, 155410 (2002); A. G. Marinopoulos, L. Reining, A. Rubio and N. Vast, Phys. Rev. Lett. **91**, 046402 (2003).
[24] M. Bruno, M. Palummo, A. Marini, R. Del Sole, and S. Ossicini, Phys. Rev. Lett. **98**, 036807 (2007); M. Palummo, R. Del Sole, V. Olevano, A. N. Kholod, and S. Ossicini, Phys. Rev. B **72**, 153310 (2005).